

Article

# Two-Dimensional Polarization Holographic Gratings in Azopolymer Thin Films: Polarization Properties in the Presence or Absence of Surface Relief

Georgi Mateev <sup>1,2</sup>, Lian Nedelchev <sup>1,2,\*</sup> , Ludmila Nikolova <sup>1</sup>, Branimir Ivanov <sup>1</sup>, Velichka Strijkova <sup>1</sup> , Elena Stoykova <sup>1</sup>, Kihong Choi <sup>3</sup>, Joongki Park <sup>3</sup> and Dimana Nazarova <sup>1,2</sup> 

<sup>1</sup> Institute of Optical Materials and Technologies, Bulgarian Academy of Sciences, 1113 Sofia, Bulgaria; georgi@iomt.bas.bg (G.M.); lnikolova@iomt.bas.bg (L.N.); branimirivanov@iomt.bas.bg (B.I.); vily@iomt.bas.bg (V.S.); estoykova@iomt.bas.bg (E.S.); dimana@iomt.bas.bg (D.N.)

<sup>2</sup> University of Chemical Technology and Metallurgy, 8 St. Kliment Ohridski Blvd, 1756 Sofia, Bulgaria

<sup>3</sup> Digital Holography Research Section, Electronics and Telecommunications Research Institute, Daejeon 34129, Republic of Korea; kihong08@etri.re.kr (K.C.); jkp@etri.re.kr (J.P.)

\* Correspondence: lian@iomt.bas.bg

**Abstract:** During polarization holographic recording in azopolymer thin films, usually together with the volume anisotropic grating, a surface relief grating (SRG) is also formed. By using two consecutive exposures, it is possible to obtain a two-dimensional (2D) grating. To the best of our knowledge, the polarization properties of such gratings have not been studied yet. To determine the influence of the surface relief on the polarization selectivity of the 2D gratings, we propose two methods to suppress the SRG formation: by varying the recording conditions or varying the sample structure. In these experiments we have used the commercially available azopolymer PAZO, poly[1-4-(3-carboxy-4-hydrophenylazo) benzene sulfonamido]-1,2-ethanediyl, sodium salt] to perform the polarization holographic recording using a 442 nm He-Cd laser. As indicated by our results, when the surface relief is present, it strongly dominates the response of the 2D grating and it behaves almost as a scalar polarization insensitive grating. Conversely, when the SRG formation is suppressed, the polarization properties of the 2D grating in all four diffracted orders are very well pronounced. In this way, we demonstrate that we can easily control SRG formation and, if desired, obtain 2D grating with high surface relief modulation, or alternatively record polarization-selective 2D gratings with virtually no surface relief.

**Keywords:** polarization holography; 2D polarization gratings; surface relief gratings; AFM; azopolymer PAZO



**Citation:** Mateev, G.; Nedelchev, L.; Nikolova, L.; Ivanov, B.; Strijkova, V.; Stoykova, E.; Choi, K.; Park, J.; Nazarova, D. Two-Dimensional

Polarization Holographic Gratings in Azopolymer Thin Films: Polarization Properties in the Presence or Absence of Surface Relief. *Photonics* **2023**, *10*, 728. <https://doi.org/10.3390/photronics10070728>

Received: 30 May 2023

Revised: 20 June 2023

Accepted: 22 June 2023

Published: 26 June 2023



**Copyright:** © 2023 by the authors. Licensee MDPI, Basel, Switzerland. This article is an open access article distributed under the terms and conditions of the Creative Commons Attribution (CC BY) license (<https://creativecommons.org/licenses/by/4.0/>).

## 1. Introduction

One of the challenges in modern photonics is the creation of increasingly complex optical elements combining different unique properties and performing multiple tasks. One example is the polarization holographic gratings (PHG) recorded in azobenzene-containing materials. A detailed overview of the properties and applications of polarization gratings and azopolymer materials can be found in [1–3]. An important property of azobenzenes is their polarization sensitivity, discovered as early as 1984 [4]. Following a series of *trans-cis-trans* isomerizations, the azobenzene chromophores reorient perpendicularly to the polarization of the recording light. During polarization holographic recording, this leads to the formation of significant spatially modulated photoinduced birefringence, which can be used to create polarization-selective elements. Additionally, it was discovered in 1995 that it is possible to induce a surface relief grating (SRG) of considerable height in azopolymers when recording polarization diffraction gratings [5,6]. In the following years, considerable efforts were made to establish the mechanism of this process [7–11]. The

process occurs at laser powers insufficient for ablation and it is believed to be based again on *trans-cis-trans* isomerization, which, in combination with a force gradient formed in the layer, redistributes the azo molecules, forming topographic structures with a sinusoidal profile. Thus, the polarization sensitivity of the material is the basis of the mass movement in azobenzene. The formed relief has a scalar nature. This is because, in a relief structure, we have a grating caused by the difference in refractive indices of the azopolymer film and air, which is much higher than the photoinduced birefringence in the azobenzene.

Various applications of the SRGs formed in azo materials have been suggested [12–16]. Using computer-generated holograms, Oscurato et al. have obtained complex surface relief structures with possible applications in the fields of surface engineering, biology, and photonics [12]. Another example we find in [13], where the effect of metal nanostructures on azopolymer after irradiation with polarized light was investigated using atomic force microscopy (AFM). Thus, SRGs are used as a non-invasive, easy-to-use microscopic method to characterize metallic nanostructures. Surface relief gratings with high diffraction efficiency have also been studied in azopolymer-based nanocomposite media with different types of nanoparticles [14–16].

Additionally, more complex, two-dimensional surface relief structures realized in azo materials have also been reported [17–22]. Yi et al. [17] show how controlling the relief height in the created two-dimensional structures can affect the formation of 3D patterns of colloids on the symmetrically and asymmetrically patterned 2D SRG substrates. The gratings were fabricated on azopolymer films by exposure to an interference pattern of Ar<sup>+</sup> laser beams. The spacing of the gratings was one and the same in both directions; however, the asymmetric 2D grating had a larger modulation depth in the vertical direction. In [18], Stiller et al. analyzed how the relief in 1D and 2D structures changes the elastic and mechanical properties of the used azopolymer (pDR1M). Additionally, using the tip of a scanning near-field optical microscope (SNOM), structures with a size of about 100 nm were inscribed onto the polymer surface. In [19], it is demonstrated how the relief formed on the azopolymer poly(Disperse orange 3) thin films can be used to easily fabricate various TiO<sub>2</sub> nanostructures for applications in photonics and electronics. Varying the angle of rotation of the substrate between the exposures from 90° to 60°, both square and hexagonal 2D SRG patterns were obtained. Huang et al. studied 2D structures created with two-step holographic recording and the dependence of surface modulation of the 2D SRG on the rotational angle between the 1D gratings for different azobenzene media [20]. Using nematic liquid crystal as an interface, it was demonstrated that the depth of the SRG groove could be enhanced about 2–3 times. The main material investigated in [21] is the azopolymer PAZO, showing the possibility to fabricate 1D and 2D SRG with an ultraviolet laser at 355 nm. Due to the short wavelength of the recording laser, gratings with a period on the order of 200 nm were obtained. The ability to reversibly generate relief structures is the main topic of research in [22]. Linearly polarized light or heat were successfully used as the stimuli for the reversible reshaping of periodic structures, imprinted in a blend of low-molecular azo glass and polystyrene.

It is very important to note, however, that the surface relief gratings (1D or 2D) in azopolymer materials coexist with an underlying volume polarization grating. In fact, for some applications, the properties of the polarization grating are more important, and the SRG has an adverse effect, deteriorating the polarization characteristics of the optical element. Examples of such applications are optical switches [23], a circular polarization beam splitter [24], bifocal polarization lenses [25], and a reconfigurable fiber Bragg filter [26], all based on azo-containing materials. In these cases, it is essential to find an efficient method to suppress the formation of the surface relief grating or to evaluate its influence on the polarization properties of the obtained holographic optical element. To the best of our knowledge however, no detailed analysis of the polarization properties of 2D gratings in the presence or absence of SRG has yet been reported.

Thus, the main goal of the present work is to investigate the polarization properties of two-dimensional polarization holographic gratings, comparing the case when an

SRG with significant height is present and the case when SRG formation is prevented. The experiments were performed using the well-known commercially available azopolymer PAZO, poly[1-4-(3-carboxy-4-hydroxyphenylazo) benzene sulfonamido]-1,2-ethanediyl, sodium salt [27–29]. Two methods of SRG suppression were employed: recording from the back (or substrate) side of the sample, for which the azopolymer layer acts as a filter reducing the intensity of light before it reaches its free surface, and enclosing the azopolymer film between two glasses when no free surface is present.

## 2. Materials and Methods

### 2.1. Samples Preparation

Thin film samples for polarization holographic recording were prepared from the commercially available azopolymer PAZO—poly[1-4-(3-carboxy-4-hydroxyphenylazo) benzenesulfonamido]-1,2-ethanediyl, sodium salt] (Sigma-Aldrich, St. Louis, Missouri, United States, #346411). The absorbance spectrum of PAZO is measured earlier [30] and is presented in Figure 1. Its chemical structure is shown in the inset.

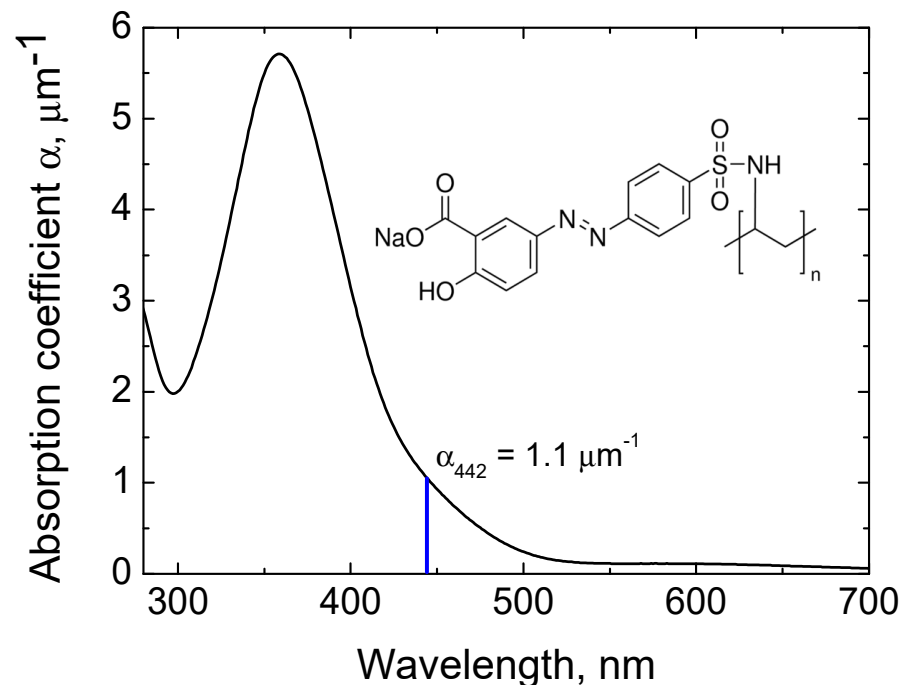


**Figure 1.** UV–Vis spectrum of the absorption coefficient of the azopolymer PAZO (adapted from [30]). The inset shows the chemical structure of PAZO.

The samples were deposited via spin-coating of PAZO/methanol solution with 100 mg/mL concentration on high-quality optical glass substrates (BK7) at 1000 rpm. The substrates are rectangular in shape and their dimensions are 24 × 36 mm. The thickness of the azopolymer layer is approximately 1800 nm, as measured by F20 Optical Thin-Film Analyzer (Filmetrics). The film thickness variation across the samples' surface is about 1%, or around 20 nm.

Additionally, we have prepared samples with a double-layer or “sandwich” structure, as shown in Figure 2c. They consist of two thin film samples bonded together with the optically transparent glue ethyl 2-cyanoacrylate (CAS No. 7085-85-0).

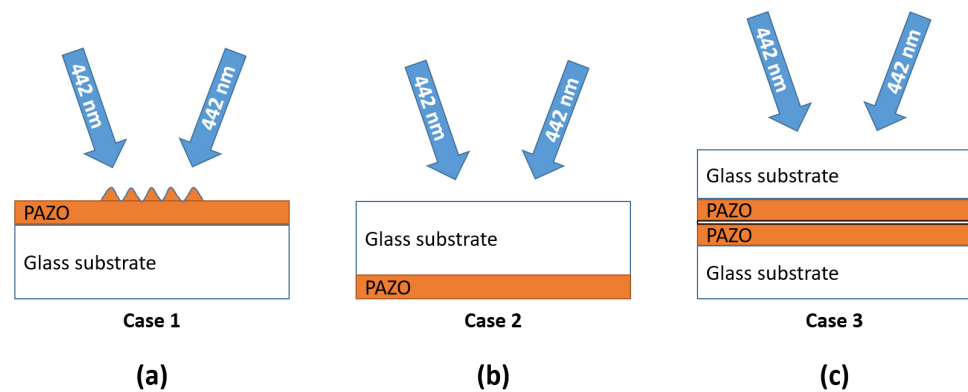


**Figure 2.** (a) Case 1—single-layer sample, recording from the azopolymer film side; (b) Case 2—single-layer sample, recording from the substrate side; (c) Case 3—double-layer “sandwich” sample.

The azopolymer films are from the inside of this sample, and the glass substrates are from the outside. In this case, two important advantages are achieved: (i) the glass slides protect the sample from mechanical damage or scratches; and (ii) there is no free surface of the azopolymer film, so the formation of surface relief grating can be effectively suppressed.

2.2. Polarization Holographic Setup

The polarization holographic recording of diffraction gratings requires the interference of two coherent light beams with wavelengths within the absorbance band of the azopolymer. In our experimental setup, illustrated in Figure 3, the coherent light source is He-Cd gas laser (IK4171I G, Kimmon Koha, Tokyo, Japan) with  $\lambda = 442 \text{ nm}$ . Using half-wave plate (HWP) and polarizing beam splitter (PBS), the laser light is split into two beams with equal intensities and by means of two quarter-wave plates (QWP), their polarizations are set to left and right circular (LCP and RCP). The resulting interference field has constant intensity, and its polarization is linear with periodically varying azimuth. These polarizations of the recording beams were selected, as it is known that, in this case, polarization holographic gratings with highest diffraction efficiency and highest surface relief modulation are obtained in azopolymers [2].

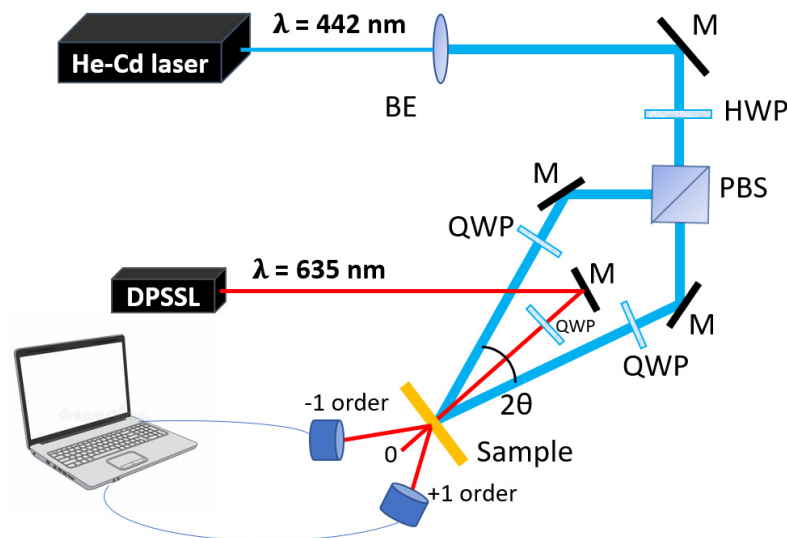


**Figure 3.** Optical setup for inscription of polarization holographic gratings. BE—beam expander, M—mirror, HWP—half-wave plate, QWP—quarter-wave plate, PBS—polarizing beam splitter, DPSSL—diode-pumped solid-state laser.

After use of the beam expander (BE), the diameter of the recording beams was 7 mm. The total light intensity on the sample was approximately  $160 \text{ mW/cm}^2$ , and the recording angle (the angle between the two recording beams, as shown in Figure 3) was  $2\theta = 20^\circ$ , which corresponds to grating period of about  $1.3 \text{ }\mu\text{m}$ . The angle,  $\theta$ , is defined as the angle between each of the recording beams and the line perpendicular to the surface of the sample. The diffraction efficiency (DE) is measured in real time during the inscription of the polarization holographic gratings, simultaneously in both +1 and -1, diffracted order, by two computer-operated power meters (PM100D, Thorlabs). The probe laser beam used to determine the DE is with left circular polarization and wavelength of 635 nm from a DPSS laser (B&W Tek Inc., Newark, Delaware, United States).

We employ three modes of recording, denoted as case 1, case 2, and case 3, as illustrated in Figure 2. In case 1, the recording is performed with the azopolymer layer facing the recording beams (Figure 2a). In this case, the intensity on the free surface of the film is maximal and this results in formation of surface relief grating. In case 2, the sample is turned back, so the substrate side is facing the recording beams (Figure 2b). The light first encounters the substrate/film interface where, due to the adhesion of the azopolymer layer to the substrate, SRG cannot form. Then, during its propagation through the azopolymer film, the intensity of light is significantly reduced due to the absorption (about 100 times for the given wavelength and sample thickness), and when it reaches the free surface of the layer, it is not sufficient to induce SRG. Finally, in case 3 (Figure 2c), there is no free azopolymer/air surface where the SRG can form.

The inscription of the 2D polarization holographic gratings is performed in two steps. First, a 1D grating is recorded until reaching saturation of the diffraction efficiency. Afterward, the sample is rotated at  $90^\circ$  counterclockwise, as shown in Figure 4a, and the recording of the second superimposed grating starts. The indices for the diffracted orders of the first grating are denoted as  $\pm 1, 0$ , while for the second grating, they are  $0, \pm 1$  (Figure 4b).

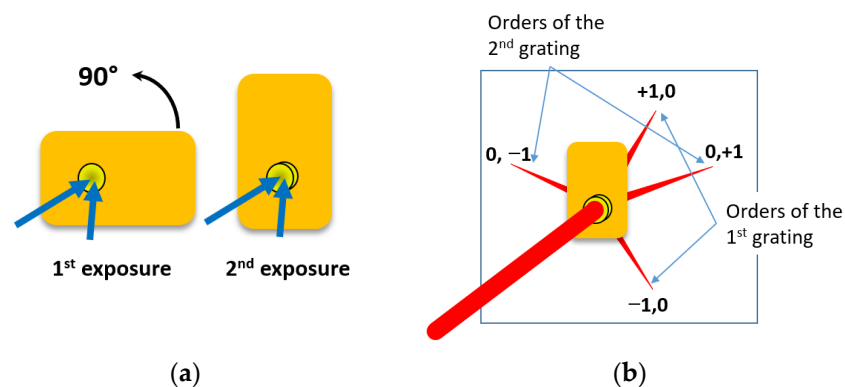


**Figure 4.** (a) Rotation of the sample between the two exposures to obtain the 2D PHG; (b) Illustration of the notations of the diffracted orders of the 2D gratings.

The inscription of the second grating reduces the diffraction efficiency of the first, so our aim is to terminate the second recording when the diffraction efficiencies of the two gratings are approximately equal. This task is even more complex because we have to take into account that the surface relief grating is more stable than the volume polarization grating.

### 2.3. Characterization of the Recorded 2D Gratings

To determine the polarization state and the diffraction efficiencies of the four diffracted orders of the 2D polarization holographic gratings, we used probe beam from a DPSS laser at 635 nm with polarization state, controlled via polarizer and quarter-wave plate (Figure 4b). The polarization incident on the sample was consecutively set to left circular (LCP), right circular (RCP), and linear, with azimuth varying from  $0^\circ$  to  $180^\circ$ . The polariza-

tion state of the  $\pm 1, 0$  and  $0, \pm 1$  diffracted orders were measured by a polarimeter (Thorlabs PAX 5710).

In order to analyze the surface topography of the gratings, we employed an atomic force microscope (Asylum Research MFP-3D, Oxford Instruments, Abingdon, UK) supplied with standard silicon probes AC160TS-R3 operating at 300 kHz with spring constant 26 N/m. For optimal visualization of the SRG features, the dimensions of the measurement area were set to  $10 \mu\text{m} \times 10 \mu\text{m}$ .

### 3. Results and Discussion

This section consists of three parts. In the first part, we present the kinetics of the DE for the  $\pm 1$  diffracted orders obtained during the inscription of the first and the second 1D grating. Next, we present the measured ellipticities and DE for all four diffracted orders of the 2D PHGs for probe light with LCP, RCP, and linear polarizations. In the last case, we also vary the input azimuth from  $0^\circ$  to  $180^\circ$ . Finally, in the third part, we use AFM analysis to obtain the parameters of the relief structures for case 1 and case 2.

#### 3.1. Diffraction Efficiency Kinetics

The diffraction efficiency kinetics for cases 1, 2, and 3 are shown in Figure 5. The main graphs correspond to the inscription of the first 1D gratings, while the insets correspond to the recording of the second 1D gratings. The polarization of the probe beam is set up to LCP. In all figures diffraction efficiency kinetics of both the +1 order ( $DE_{+1}$ ) and the -1 order ( $DE_{-1}$ ) are plotted.

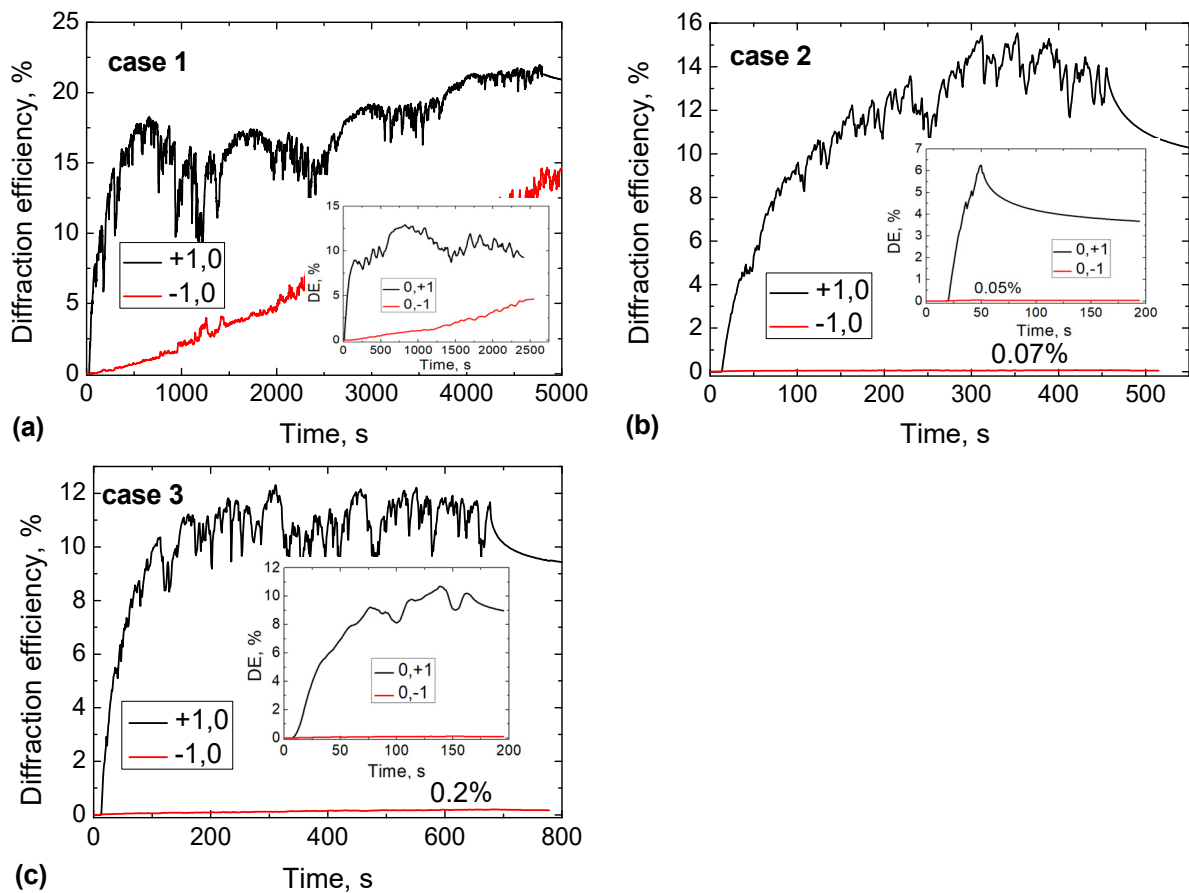


**Figure 5.** Kinetics of the DE for the first 1D grating in both +1 and -1 diffracted orders for case 1 (a), case 2 (b), and case 3 (c). The insets present the DE kinetics for the second grating recording.

Here, we analyze in detail the data presented in Figure 5. It is well known from the theory of polarization holography [2], that when a polarization grating, recorded with left and right circularly polarized beams, is illuminated with circularly polarized light, the light will be directed only in the +1 order of diffraction. In case 1, however, we observe significant diffraction also in the −1 order, both for the first and second grating. This clearly indicates the formation of surface relief grating. Because of its scalar nature, the SRG distributes light equally in +1 and −1 orders. On the other hand, the fast increase in  $DE_{+1}$  at the beginning of the recording and the fact that the value of  $DE_{+1}$  is higher than  $DE_{-1}$  prove that a volume polarization grating is also present. Still, the ratio of the maximal diffraction efficiencies for the  $\pm 1$  orders,  $DE_{-1\max}/DE_{+1\max} = 65\%$ , indicates that the SRG has a more significant contribution to the total DE in comparison with the polarization grating. The noticeable fluctuations of the kinetic curve  $DE_{+1}(t)$  are due not only to external factors but also to the change in the polarizations of the recording beams caused by the surface grating. This issue will be discussed in more detail in our forthcoming article.

In contrast, in case 2 and case 3, the ratio  $DE_{-1\max}/DE_{+1\max}$  is negligible (about or even below 1%). Hence, we can conclude that in these two cases, the formation of the surface relief grating was efficiently suppressed. The absence of SRG leads to a lower value of the maximal DE compared to case 1, but at the same time significantly improves the polarization properties of the PHG, as will be demonstrated in the next section.

We should also note that the recording time of the second grating is shorter than the recording time of the first grating. The first grating is recorded until saturation of  $DE_{+1}$  is reached, while the recording of the second grating is stopped when its DE is approximately the same as that of the first one.

### 3.2. Polarization Properties of the 2D Gratings

After the inscription of the 2D polarization holographic gratings, their polarization properties were evaluated using the method described in Section 2.3. Generally, we could expect the behavior of each couple of diffracted orders of the 2D polarization holographic grating (+1, 0 and −1, 0; 0, +1 and 0, −1) to be similar to that of the orders of the 1D grating. The dependencies of the diffraction efficiency and ellipticity for all four diffracted orders on the azimuth,  $\varphi$ , of a linearly polarized probe beam are presented in Figure 6.

If we consider the ellipticity vs. azimuth dependences, we can see that the presence of the surface relief in case 1 significantly influences the polarization properties of the 2D grating. The average value of the ellipticity is approximately zero (or linear, as is the polarization of the probe beam) due to the dominance of the SRG, with a modulation of about 0.3. On the other hand, in case 2 and case 3 where the surface relief grating is absent, we observe a very clear distinction between the ellipticity of the diffracted orders: two of them are close to RCP, and the other two are close to LCP. These characteristics are typical for polarization-selective grating.

The variation of the diffraction efficiency on the input azimuth in case 1 is most pronounced for the 0, +1 order, and it is in the range 7–11.5%. The DE values in case 1 are higher than in case 2 and case 3, and this can be ascribed to the presence of SRG, which contributes to the DE. We should also note that in case 2 and case 3, there is no significant modulation for three of the diffracted orders.

Table 1 summarizes the experimental data on the diffraction efficiency and the output ellipticity ( $e_{\text{out}}$ ) of the four diffracted orders when the probe laser beam has left circular polarization ( $e_{\text{in}} = -1$ ) or right circular polarization ( $e_{\text{in}} = +1$ ).

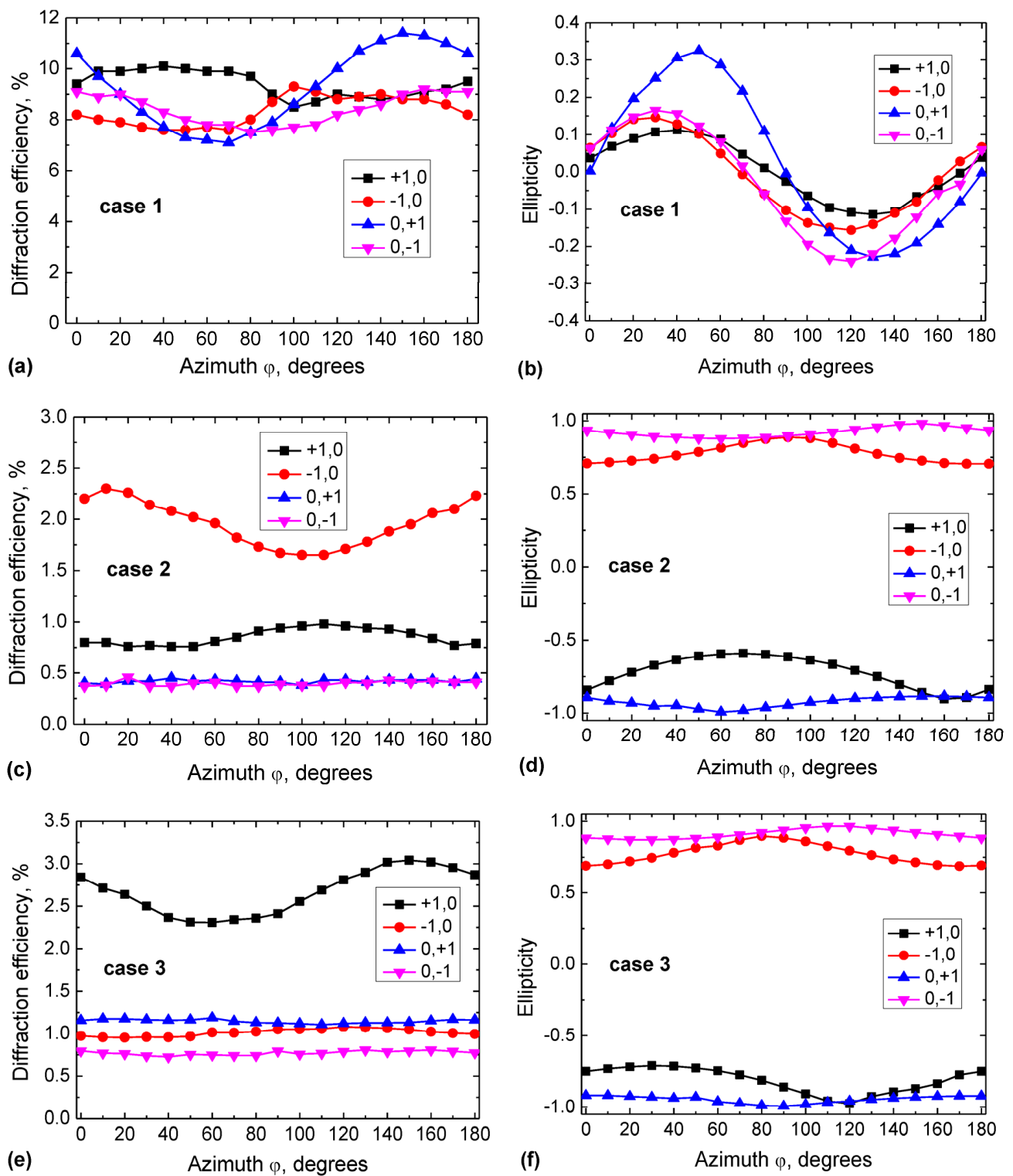


**Figure 6.** Dependencies of the diffraction efficiency (a,c,e) and ellipticity (b,d,f) for all four diffracted orders of the 2D grating on the azimuth,  $\varphi$ , of a linearly polarized probe beam. (a,b) Correspond to case 1; (c,d) to case 2; (e,f) to case 3.

**Table 1.** Experimental data for DE and  $e_{out}$  for cases 1, 2, and 3 for LCP and RCP probe light ( $e_{in} = \pm 1$ ).

$e_{in}$	Diffr. Order	Case I		Case II		Case III	
		$e_{out}$	DE, %	$e_{out}$	DE, %	$e_{out}$	DE, %
−1	+1,0	−0.72	10.4	0.84	4.0	0.94	2.5
−1	−1,0	−0.77	5.5	-	0.2	0.68	0.5
−1	0, +1	−0.67	10.7	0.90	1.6	0.95	2.6
−1	0, −1	−0.62	6.8	-	0.02	-	0.2
+1	+1, 0	0.86	12.2	-	0.3	−0.94	0.1
+1	−1, 0	0.87	7.1	−0.83	2.7	−0.78	2.0
+1	0, +1	0.90	12.1	-	0.01	-	0.1
+1	0, −1	0.83	10.5	−0.97	1.2	−0.88	4.7

As seen from the data in Table 1, in case 1, the output ellipticity for all orders has the same sign as the input ellipticity. This fact again confirms the presence of the scalar surface relief grating. The total diffraction efficiency (the sum of the DE for all four orders), however, is relatively high: for the RCP probe light, it is  $DE_{total} = 41.9\%$ .

In contrast, for case 2 and case 3, we observe the typical behavior of a polarization-selective grating: the LCP probe light ( $e_{in} = -1$ ) is diffracted mainly in the +1, 0 and 0, +1 orders, while the RCP probe light ( $e_{in} = +1$ ) is diffracted in the −1, 0 and 0, −1 orders. At the same time, the ellipticity of the diffracted orders ( $e_{out}$ ) is with reverse sign compared to the input ellipticity. The high polarization selectivity of the gratings in cases 2 and 3 is also the reason for the missing values of the output ellipticity for some of the diffracted orders: the light intensity is so low that it is not possible to obtain reliable data using the polarimeter. We should also note that for case 2 and case 3, the ratio between the diffraction efficiency in the +1 and −1 order ( $DE + 1/DE - 1$ ) is higher for the second gratings than for the first ones. A possible explanation is that the inscription of the second polarization grating reduces the polarization selectivity of the first.

### 3.3. Atomic Force Microscopy Analysis

Using AFM, we have analyzed the surface topography of the 2D holographic gratings, recorded in case 1 and case 2. In case 3, the azopolymer layer is covered from both sides with glass slides and there is no free film surface to be studied by AFM. The results are shown in Figure 7.

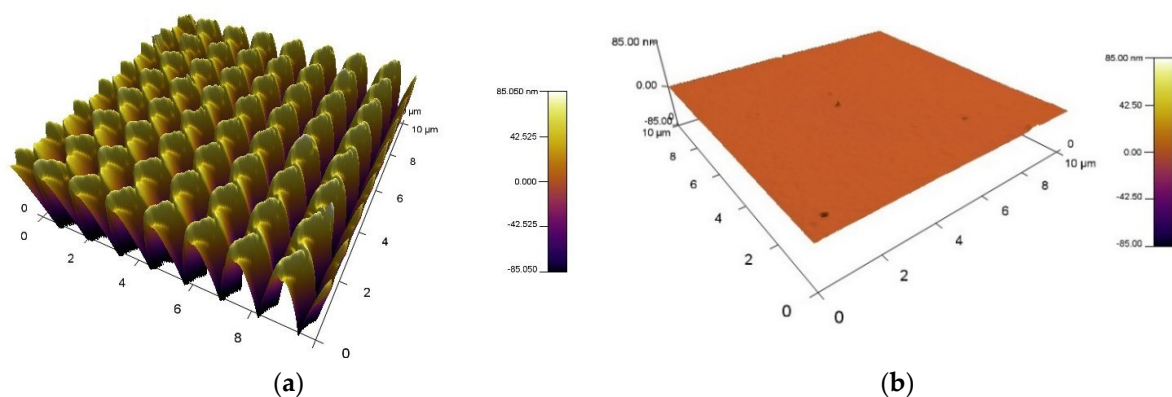


**Figure 7.** (a) AFM image of the 2D grating in case 1, where a significant surface relief is present; (b) AFM image of the 2D grating in case 2, where the SRG formation is suppressed. The scale of the color bars is from −85 nm to +85 nm.

In case 1 (Figure 7a), a periodic two-dimensional surface relief structure is clearly observed with a period of  $1.3 \times 1.3 \mu\text{m}$  and a height of about 170 nm. This fully corresponds to the already presented data about the diffraction efficiency and polarization properties of this type of grating. Figure 7b is plotted on the same scale and depicts case 2. No periodic modulation of the surface can be seen, and the maximal height is below 5 nm, which corresponds to the typical surface roughness of a non-recorded azopolymer film. This demonstrates that for case 2, SRG formation has been successfully prevented.

#### 4. Conclusions

We have recorded two-dimensional polarization holographic gratings in thin azopolymer films and studied their polarization properties and surface topography. Three different modes of recording were employed. In case 1, the azopolymer film was facing the recording beams. As a result, 2D surface relief grating was formed with a height of about 170 nm. The total diffraction efficiency in this case reached 42%. However, the polarization selectivity of the grating was low, as the scalar SRG had a more significant contribution than the volume polarization grating. On the other hand, by recording from the substrate side of the sample (case 2) or using a “sandwich” sample, covered with glass from both sides (case 3), we successfully suppressed the formation of SRG and obtained gratings with high polarization selectivity. Therefore, using the same optical setup and simply flipping the sample, we can easily obtain 2D polarization holographic gratings either with significant surface relief or with high polarization selectivity.

**Author Contributions:** Conceptualization, L.N. (Lian Nedelchev), L.N. (Ludmila Nikolova) and D.N.; methodology, G.M.; validation, L.N. (Lian Nedelchev) and D.N.; formal analysis, K.C. and J.P.; investigation, G.M., B.I. and V.S.; writing—original draft preparation, G.M.; writing—review and editing, L.N. (Lian Nedelchev); visualization, G.M.; supervision, L.N. (Lian Nedelchev) and D.N.; funding acquisition, L.N. (Lian Nedelchev) and E.S. All authors have read and agreed to the published version of the manuscript.

**Funding:** This work was supported by the Institute of Information & Communications Technology Planning & Evaluation (IITP), grant No. 2019-0-00001. G. Mateev acknowledges the financial support from the Bulgarian Ministry of Education and Science under the National Research Programme “Young scientists and postdoctoral students-2”, approved by DCM 206/07.04.2022. L. Nedelchev and D. Nazarova are grateful for the funding from the European Union—NextGenerationEU, through the National Recovery and Resilience Plan of the Republic of Bulgaria, project № BG-RRP-2.004-0002, “BiOrgaMCT”.

**Institutional Review Board Statement:** Not applicable.

**Informed Consent Statement:** Not applicable.

**Data Availability Statement:** All data generated or analyzed during this study are included in this published article.

**Conflicts of Interest:** The authors declare no conflict of interest. The funders had no role in the design of the study; in the collection, analyses, or interpretation of data; in the writing of the manuscript; or in the decision to publish the results.

#### References

1. Natansohn, A.; Rochon, P. Photoinduced Motions in Azo-Containing Polymers. *Chem. Rev.* **2002**, *102*, 4139–4175. [[CrossRef](#)]
2. Nikolova, L.; Ramanujam, P.S. *Polarization Holography*; Cambridge University Press: Cambridge, UK, 2009. [[CrossRef](#)]
3. Wang, X. *Azo Polymers: Synthesis, Functions and Applications*; Springer: Berlin/Heidelberg, Germany, 2017. [[CrossRef](#)]
4. Todorov, T.; Nikolova, L.; Tomova, N. Polarization holography. 1: A new high-efficiency organic material with reversible photoinduced birefringence. *Appl. Opt.* **1984**, *23*, 4309–4312. [[CrossRef](#)]
5. Rochon, P.; Batalla, E.; Natansohn, A. Optically induced surface gratings on azoaromatic polymer films. *Appl. Phys. Lett.* **1995**, *66*, 136–138. [[CrossRef](#)]
6. Kim, D.Y.; Tripathy, S.K.; Li, L.; Kumar, J. Laser-induced holographic surface relief gratings on nonlinear optical polymer films. *Appl. Phys. Lett.* **1995**, *66*, 1166–1168. [[CrossRef](#)]

7. Kumar, J.; Li, L.; Jiang, X.L.; Kim, D.Y.; Lee, T.S.; Tripathy, S. Gradient force: The mechanism for surface relief grating formation in azobenzene functionalized polymers. *Appl. Phys. Lett.* **1998**, *72*, 2096–2098. [[CrossRef](#)]
8. Barrett, C.J.; Rochon, P.; Natansohn, A. Model of laser-driven mass transport in thin films of dye-functionalized polymers. *J. Chem. Phys.* **1998**, *109*, 1505–1516. [[CrossRef](#)]
9. Baldus, O.; Leopold, A.; Hagen, R.; Bieringer, T.; Zilker, S.J. Surface relief gratings generated by pulsed holography: A simple way to polymer nanostructures without isomerizing side-chains. *J. Chem. Phys.* **2001**, *114*, 1344–1349. [[CrossRef](#)]
10. Bublitz, D.; Fleck, B.; Wenke, L. A model for surface-relief formation in azobenzene polymers. *Appl. Phys. B* **2001**, *72*, 931–936. [[CrossRef](#)]
11. Pedersen, T.G.; Johansen, P.M.; Holme, N.C.R.; Ramanujam, P.S.; Hvilsted, S. Mean-field theory of photoinduced formation of surface reliefs in side-chain azobenzene polymers. *Phys. Rev. Lett.* **1998**, *80*, 89–92. [[CrossRef](#)]
12. Oscurato, S.L.; Salvatore, M.; Borbone, F.; Maddalena, P.; Ambrosio, A. Computer-generated holograms for complex surface reliefs on azopolymer films. *Sci. Rep.* **2019**, *9*, 6775. [[CrossRef](#)]
13. Hubert, C.; Romyantseva, A.; Lerondel, G.; Grand, J.; Kostcheev, S.; Billot, L.; Vial, A.; Bachelot, R.; Royer, P.; Chang, S.H.; et al. Near-field photochemical imaging of noble metal nanostructures. *Nano Lett.* **2005**, *5*, 615–619. [[CrossRef](#)]
14. Nedelchev, L.; Mateev, G.; Strijkova, V.; Salgueiriño, V.; Schmool, D.S.; Berberova-Buhova, N.; Stoykova, E.; Nazarova, D. Tunable Polarization and Surface Relief Holographic Gratings in Azopolymer Nanocomposites with Incorporated Goethite ( $\alpha$ -FeOOH) Nanorods. *Photonics* **2021**, *8*, 306. [[CrossRef](#)]
15. Stoilova, A.; Mateev, G.; Nazarova, D.; Nedelchev, L.; Stoykova, E.; Blagoeva, B.; Berberova, N.; Georgieva, S.; Todorov, P. Polarization holographic gratings in PAZO polymer films doped with particles of biometals. *J. Photochem. Photobiol. A Chem.* **2021**, *411*, 113196. [[CrossRef](#)]
16. Berberova-Buhova, N.; Nedelchev, L.; Mateev, G.; Stoykova, E.; Strijkova, V.; Nazarova, D. Influence of the size of Au nanoparticles on the photoinduced birefringence and diffraction efficiency of polarization holographic gratings in thin films of azopolymer nanocomposites. *Opt. Mater.* **2021**, *121*, 111560. [[CrossRef](#)]
17. Yi, D.K.; Seo, E.M.; Kim, D.Y. Surface-modulation-controlled three-dimensional colloidal crystals. *Appl. Phys. Lett.* **2002**, *80*, 225–227. [[CrossRef](#)]
18. Stiller, B.; Geue, T.; Morawetz, K.; Saphiannikova, M. Optical patterning in azobenzene polymer films. *J. Microsc.* **2005**, *219*, 109–114. [[CrossRef](#)]
19. Kim, S.S.; Chun, C.; Hong, J.C.; Kim, D.Y. Well-ordered TiO<sub>2</sub> nanostructures fabricated using surface relief gratings on polymer films. *J. Mater. Chem.* **2006**, *16*, 370–375. [[CrossRef](#)]
20. Huang, B.Y.; Yu, K.Y.; Huang, S.Y.; Kuo, C.T. The investigation of the two-dimensional surface relief grating on dye-doped polymer film. *Opt. Mater. Express* **2014**, *4*, 308–314. [[CrossRef](#)]
21. Sakhno, O.; Goldenberg, L.M.; Wegener, M.; Dreyer, C.; Berdin, A.; Stumpe, J. Generation of sub-micrometer surface relief gratings in an azobenzene-containing material using a 355 nm laser. *Opt. Mater.* **2022**, *128*, 112457. [[CrossRef](#)]
22. Kaban, B.; Bagatur, S.; Soter, M.; Hillmer, H.; Fuhrmann-Lieker, T. Reversible Photo-Induced Reshaping of Imprinted Microstructures Using a Low Molecular Azo Dye. *Polymers* **2022**, *14*, 586. [[CrossRef](#)]
23. Ikeda, T.; Tsutsumi, O. Optical switching and image storage by means of azobenzene liquid-crystal films. *Science* **1995**, *268*, 1873–1875. [[CrossRef](#)]
24. Nedelchev, L.; Todorov, T.; Nikolova, L.; Petrova, T.; Tomova, N.; Dragostinova, V. Characteristics of high-efficient polarization holographic gratings. *Proc. SPIE* **2001**, *4397*, 338–342. [[CrossRef](#)]
25. Nedelchev, L.; Mateev, G.; Nikolova, L.; Nazarova, D.; Ivanov, B.; Strijkova, V.; Stoykova, E.; Choi, K.; Park, J. In-line and off-axis polarization-selective holographic lenses recorded in azopolymer thin films via polarization holography and polarization multiplexing. *Appl. Opt.* **2023**, *62*, D1–D7. [[CrossRef](#)]
26. Lausten, R.; Rochon, P.; Ivanov, M.; Cheben, P.; Janz, S.; Desjardins, P.; Ripmeester, J.; Siebert, T.; Stolow, A. Optically reconfigurable azobenzene polymer-based fiber Bragg filter. *Appl. Opt.* **2005**, *44*, 7039–7042. [[CrossRef](#)]
27. Minkov, D.; Nedelchev, L.; Angelov, G.; Marquez, E.; Blagoeva, B.; Mateev, G.; Nazarova, D. Hybrid dispersion model characterization of PAZO polymer thin films over the entire transmittance spectrum measured in the UV/VIS/NIR spectral region. *Materials* **2022**, *15*, 8617. [[CrossRef](#)]
28. Nedelchev, L.; Nazarova, D.; Mateev, G.; Berberova, N. Birefringence induced in azopolymer (PAZO) films with different thickness. *Proc. SPIE* **2015**, *9447*, 94471I. [[CrossRef](#)]
29. Yadavalli, N.S.; Santer, S. In-situ atomic force microscopy study of the mechanism of surface relief grating formation in photosensitive polymer films. *J. Appl. Phys.* **2013**, *113*, 224304. [[CrossRef](#)]
30. Nedelchev, L.; Ivanov, D.; Berberova, N.; Strijkova, V.; Nazarova, D. Polarization holographic gratings with high diffraction efficiency recorded in azopolymer PAZO. *Opt. Quantum Electron.* **2018**, *50*, 212. [[CrossRef](#)]

**Disclaimer/Publisher’s Note:** The statements, opinions and data contained in all publications are solely those of the individual author(s) and contributor(s) and not of MDPI and/or the editor(s). MDPI and/or the editor(s) disclaim responsibility for any injury to people or property resulting from any ideas, methods, instructions or products referred to in the content.